IJE TRANSACTIONS A: Basics Vol. 30, No. 7, (July 2017) 1054-1065

International Journal of Engineering

Journal Homepage: www.ije.ir

Slip Velocity in Flow and Heat Transfer of Non-newtonian Fluids in Microchannels

A. H. Sarabandi, A. Jabari Moghadam*

Mechanical Engineering Department, Shahrood University of Technolgy, Shahrud, Iran

P A P E R I N F O

Paper history:
Received 22 December 2016
Received in revised form 02 March 2017
Accepted 21 April 2017

Keywords:
Heat Transfer
Non-Newtonian Fluids
Slip
Brinkman Number
Analytic Solution
Entropy Generation
Nusselt Number

A B S T R A C T

The steady-state fully-developed laminar flow of non-Newtonian power-law fluids is examined in a circular microchannel with slip boundary condition and under an imposed constant wall heat flux. Effects of slip as well as the hydrodynamic and thermal key parameters on heat transfer and entropy generation are investigated. The results reveal that increasing the Brinkman number and the flow behavior index both lead to increasing the entropy generation and decreasing the Nusselt number. In heating process, the temperature difference between the fluid and the wall decreases as the slip coefficient increases; similar trend may or may not be observed for cooling process, determined by the range of the slip coefficient as well as the Brinkman number. An increase in the slip coefficient leads to an increase in both the Nusselt number and the Bejan number, whereas it gives rise to a decrease in entropy generation. For each particular value of the slip coefficient, the Nusselt number approaches a specific value as the Brinkman number and/or the flow behavior index increases. An increase in the flow behavior index or a decrease in the slip coefficient results in incrementing the average entropy generation.

***doi**: 10.5829/ije.2017.30.07a.15*

1. INTRODUCTION

For liquid flows in macro scale, no-slip boundary condition on solid surface is widely assumed, which may not be always correct in micro and nano fluidic systems. Recent experimental studies of microflows revealed that boundary conditions at the channel wall depend on both flow length scale and surface properties. Hydrophobic smooth surfaces such as in polydimethylsiloxane (PDMS materials) made channels [1-3]. Analysis of heat and fluid flow at microscale is of great importance not only for playing a key rule in the biological systems, but also for its application in cooling of electronic equipments [4]. Liquid slip can occur even when the continuum hypothesis is perfectly valid [5]. It is well studied that boundary slip is often characterized by slip length, which is defined as the distance between the surface and the point inside the surface at which the extrapolated velocity of the fluid equals to zero. Liquid molecules exist in a state of continual collision. Their behavior is completely different from that of gases and is significantly more complex; the molecular theory of liquids is not as well developed as that for gases. There are no parameters such as Knudsen number to help in determining the regime in which a liquid might be [6]. Afonso et al. [7] performed analytic solution for viscoelastic fluids under the mixed influence of electrokinetic and pressure forces in micron sized ducts. Ashorynejad et al. [8] used Parameterized Perturbation Method to obtain the solution of momentum and heat transfer equations of non-Newtonian fluid flow in channel with porous wall. They found that the increment in the Reynolds number has similar effects on velocity components, both of them increased. Chiu and cheng [9] performed an analytical model for electrokinetic flow of power-law fluid through a slit channel. Thay observed that in the presence of an applied pressure gradient, the power-law rheology becomes more influential on the flow, despite the Newtonian depletion layer. Bharti et al. [10] studied numerically the electroviscous effect of power-law fluids through a uniform cylindrical microchannel by solving the Poisson-Boltzmann and momentum equation. Dehkordi and Mohammadi [11] performed a numerical investigation on the transient behavior of a

*Corresponding Author's Email: *alijabari@shahroodut.ac.ir* (A. Jabari Moghadam)

Please cite this article as: A. H. Sarabandi, A. Jabari Moghadam, Slip Velocity in Flow and Heat Transfer of Non-newtonian Fluids in Microchannels, TRANSACTIONS A: Basics Vol. 30, No. 7, (July 2017) 1054-1065

fully-developed flow of a laminar power-law fluid, taking into account the effect of viscous dissipation. Barkhordari and Etemad [12] conducted a numerical study on convective heat transfer of non-Newtonian fluid flows in microchannels at both constant temperature and constant heat flux boundary conditions in the absence of viscous dissipation. Their computational results showed that a change in the slip coefficient decreased Poiseuille number while increasing local Nusselt number. Tyagi [13] performed a wide study on the effect of viscous dissipation on the fully developed laminar forced convection in cylindrical tubes with an arbitrary cross-section and uniform wall temperature. Rao and Rajagopal [14] investigated the consequences of slip at the wall on the flow of a linearly viscous fluid in a channel. Since there are many practical applications related to non-Newtonian fluids, the assessment of the heat transfer characteristics is vital for accomplishing successful thermal designs. An analysis of laminar forced convection in a pipe for a Newtonian fluid with constant properties was performed by Aydin [15]. The temperature distribution and Nusselt number were analytically determined as a function of the Brinkman number by taking the viscous dissipation into account. Tso et al. [16] investigated the effect of viscous dissipation on the heat transfer for a power-law fluid between fixed parallel plates and compared the heat transfer for pseudo-plastic and dilatant fluids. Lawal [17] performed an analytical study of forced convection heat transfer of power-law fluids in four geometric shapes including trapezoidal, triangular, circular and square ducts. Hung [18, 19] investigated an analytical study on the forced convection laminar fully-developed flow of constant property nanofluids in microchannels. Chen et al. [20] studied heat transfer characteristics of power-law fluid flow in a microchannel and presented dimensionless temperature distributions and fully developed Nusselt numbers for different parameters such as flow behavior index, ratio of Debye length to half channel height, ratio of Joule heating to surface heat flux, and Brinkman number. Moghadam [21, 22] recently studied the electrokinetic flow and associated heat transfer of Newtonian fluids in microchannels with different shapes and under various imposed external body forces. Also, Moghadam [23] presented an analytical analysis on non-Newtonian power-law fluids in a circular microchannel to get analytical expressions for velocity and temperature profiles, the friction coefficient, and the fully-developed Nusselt number in the electroosmotic flow. Mohammadi and Moghadam [24] performed an analytic analysis on thermal characteristics of Bingham plastic fluids in circular microchannels; they obtained closed-form expressions for important variables in related heat transfer and entropy generation. Also, Sarabandi and Moghadam [25] examined flow and heat transfer of power-law fluids in circular microchannels. Larrode et al. [26] studied the influence of rarefaction on heat transfer in circular tubes for slip flow. Moghadam and Akbarzadeh [27] studied the effect of alternating current electric field on electroosmotic flow of non-Newtonian power-law fluids in microchannels. Also, two-fluid electroosmotic flow in a microchannel has been examined by Moghadam [28]. Bejan [29-31] has focused on the different reasons behind entropy generation in applied thermal engineering. He also presented entropy generation minimization (EGM) in different cases, compared them together and discussed its derivations and applications in a vast coverage of applied thermal engineering. Mah et al. [32] studied the effect of viscous dissipation on entropy generation in laminar fully-developed forced convection for a nanofluid (water-alumina) and compared the results for two models. Entropy generation for a non-Newtonian fluid in microchannels was studied by Tan and chen [33], Hung [34] and Mahmud and Fraser [35, 36]. They analyzed the effects of viscous dissipation and non-Newtonian behavior on entropy generation for a forced convective heat transfer in a microchannel between parallel plates for a power-law fluid. Mahmud and Fraser [37] represented a comparison study for power-law fluids for two geometries. The entropy generation rate in a purely electroosmotic flow of a non-Newtonian fluid in a parallel flat plate microchannel was studied by Escandon et al. [38].

2. PROBLEM DESCRIPTION

Hydrodynamically and thermally developed flow of power-law non-Newtonian fluids with constant properties are analyzed under an imposed wall heat flux in a circular microchannel (Figure 1).

The steady-state fully-developed flow of a power-law fluid is considered in a circular microchannel [38, 39]:

$$\frac{\partial}{\partial r}\left(r\, m\left(-\frac{dV_z}{dr} \right)^n \right) = -r\frac{\partial p}{\partial z} \tag{1a}$$

$$V_z\left(r = r_0\right) = V_s \quad , \quad \frac{dV_z}{dr}\left(r = 0\right) = 0 \tag{1b}$$

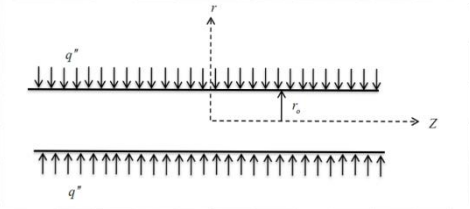

Figure1. Schematic of the physical model

where, m and n are the consistency factor and the power-law index, respectively; r_0 is the channel radius and V_s is the slip velocity on the wall. The slip boundary condition can be implemented via the slightly more intuitive idea of a slip length. If the fluid velocity at the boundary is non-zero, the slip-length is simply the extrapolation of the (linear) velocity gradient to zero, beyond the boundary condition is evaluated at the surface in which l is called the slip-length and subscript s stands for the fluid properties at the surface [40]. In additin, another slip boundary condition applicable to non-Newtonian fluids is the non-linear Navier slip boundary condition, at which the wall velocity is proportional to the velocity gradient $V_s = -l\left(dV_z/dr\right)_{r=r_o}$ [41]. The following dimensionless quantities:

$$R=\frac{r}{r_o}, Z=\frac{z}{r_o}, V=\frac{V_z}{V_m}, \beta=V_s^*=\frac{V_s}{V_m},$$
$$L=\frac{l}{r_o}, P=\frac{p}{\rho V_m^{\,2}}, Re=\frac{\rho V_m^{\,2-n} r_o^{\,n}}{m}, \tau_{rz}=m\left(-\frac{dV_z}{dr}\right)^n \quad (2)$$

are now introduced to nondimensionalize the momentum equation and its boundary conditions (1):

$$\frac{d}{dR}\left(R\left(-\frac{dV}{dR}\right)^n\right)=-Re\,R\frac{\partial P}{\partial Z} \quad (3a)$$

$$V\left(R=1\right)=V_s^*=\beta \;,\; \frac{dV}{dR}\left(R=0\right)=0 \quad (3b)$$

in which, Re is Reynolds number, L is dimensionless slip length, and β is slip coefficient. Solution of Equation (3) is:

$$V=\left(\frac{n}{n+1}\right)\left(-\frac{Re}{2}\frac{\partial P}{\partial Z}\right)^{\frac{1}{n}}\left(1-R^{\frac{n+1}{n}}\right)+\beta \quad (4)$$

where, the Reynolds number for power-law fluids is defined as:

$$\mathrm{Re}=\frac{\rho \bar{V}_z^{(2-n)} D_h^{\,n}}{m} \quad (5)$$

The critical Reynolds number for power-law fluids defined as follows [42]:

$$\mathrm{Re}_c=\frac{6464n}{(3n+1)^2}(2+n)^{\left(\frac{2+n}{1+n}\right)} \quad (6)$$

For a fixed volumetric flow rate $\left(\int_0^1 VRdR = 1/2\right)$, the dimensionless average velocity V_m may be obtained; and with the help of Equation (4), we have:

$$\frac{\partial P}{\partial Z}=-\frac{2}{Re}\left(\frac{3n+1}{n}(1-\beta)\right)^n \quad (7)$$

Hence, the dimensionless velocity distribution in Equation (4) is written as:

$$V=\frac{3n+1}{n+1}(1-\beta)\left(1-R^{\frac{n+1}{n}}\right)+\beta \quad (8)$$

The dimensionless slip boundary condition becomes:

$$\beta=-L\left(\frac{dV}{dR}\right)_{R=1}=\frac{L(3n+1)}{n+L(3n+1)} \quad (9)$$

Poiseuille number is a dimensionless parameter that indicates the resistance between fluid and microchannel wall, and is expressed as:

$$Po = f\,\mathrm{Re} \quad (10)$$

in which, f is Darcy friction coefficient [43]:

$$f=\frac{2\tau_{rz(r=r_o)}}{\rho \bar{V}_z^{\,2}} \quad (11)$$

Using Equations (2), (5), and (11), the Poiseuille number for Power-law fluids is derived as:

$$Po=2^{n+1}\left(\frac{3n+1}{n}\right)^n \quad (12)$$

For fully-developed flow of a constant-property liquid in a circular microchannel, the energy equation is expressed as [38, 39]:

$$\rho C_p V_z r\frac{\partial T}{\partial z}=k\frac{\partial}{\partial r}\left(r\frac{\partial T}{\partial r}\right)+rm\left(-\frac{dV_z}{dr}\right)^{n+1} \quad (13)$$

where, T is temperature, ρ, C_p and k are the fluid density, specific heat, and thermal conductivity, respectively [23]. The thermal boundary conditions in non-dimensional form are:

$$\left(\frac{\partial T}{\partial r}\right)_{r=0}=0 \;,\; \left(k\frac{\partial T}{\partial r}\right)_{r=r_o}=q'' \quad (14)$$

where, q'' is the wall heat flux. The bulk temperature T_m is defined as [43]:

$$T_m=\frac{2}{r_o^2 V_m}\int_0^{r_o} V_z T\, r\, dr \;;\; \left(\text{in this case, } \frac{\partial T}{\partial z}=\frac{\partial T_m}{\partial z}\right) \quad (15)$$

Integrating Equation (13) over the cross-sectional area [32]:

$$\rho C_p \frac{\partial}{\partial z}\int_0^{r_o} V_z T r dr=\left(kr\frac{\partial T}{\partial r}\right)_0^{r_o}+m\int_0^{r_o} r\left(-\frac{dV_z}{dr}\right)^{n+1} dr \quad (16)$$

and utilizing Equations (14) and (15), we get:

$$\frac{\partial T_m}{\partial z}=\frac{2}{pc_p r_o^2 V_m}\left(q'' r_o+m\left(V_m(1-\beta)\right)^{n+1}\left(\frac{3n+1}{n}\right)^n r_o^{\,1-n}\right) \quad (17)$$

The dimensionless temperature and the Brinkman number (the relative importance of viscous heat generation to external heating) are defined as follows:

$$\theta=\left(T-T_w\right)\Big/\left(\frac{q''D_h}{k}\right),\quad Br=mD_h\left(\frac{V_m}{D_h}\right)^{n+1}\Big/q'' \quad (18)$$

The positive and negative values of Br refer to wall heating (fluid is being heated) and wall cooling (fluid is being cooled), respectively. The energy Equation (13) in non-dimensional form becomes:

$$\frac{1}{R}\frac{\partial}{\partial R}\left(R\frac{\partial\theta}{\partial R}\right)=V\left(1+2^n Br(1-\beta)^{n+1}\left(\frac{3n+1}{n}\right)^n\right) -\left(2^{n-1}Br(1-\beta)^{n+1}\left(\frac{3n+1}{n}\right)^{n+1}R^{\frac{n+1}{n}}\right) \tag{19}$$

The dimensionless thermal boundary conditions are:

$$\left(\frac{\partial\theta}{\partial R}\right)_{R=0}=0\ ,\ \theta(R=1)=0 \tag{20}$$

Solution of Equation (19) with respect to (20) is:

$$\theta(R)=\left(\begin{array}{l}\left(1+2^n Br(1-\beta)^{n+1}\left(\frac{3n+1}{n}\right)^n\right)\left[\begin{array}{l}\frac{R^2}{4}\left(\frac{3n+1}{n+1}(1-\beta)+\beta\right)\\ -\frac{n^2(1-\beta)}{(n+1)(3n+1)}R^{\frac{3n+1}{n}}\\ -\left(\frac{3n+1}{n+1}\right)(1-\beta)\left(\frac{1}{4}-\left(\frac{n}{3n+1}\right)^2-\frac{\beta}{4}\right)\end{array}\right]+\\ \left(2^{n-1}Br(1-\beta)^{n+1}\left(\frac{3n+1}{n}\right)^{n-1}\left(1-R^{\frac{3n+1}{n}}\right)\right)\end{array}\right) \tag{21}$$

Nusselt number is analytically obtained as:

$$Nu=\frac{-1}{2\int_0^1 VR\,\theta\,dR}$$

$$=\frac{8(n+1)^2(15n^2+8n+1)}{\begin{array}{l}1+14n+2^nBr\left(\frac{3n+1}{n}\right)^n(1-\beta)^n+28\beta^2n^22^nBr\left(\frac{3n+1}{n}\right)^n(1-\beta)^n\\ -14\beta nBr2^n\left(\frac{3n+1}{n}\right)^n(1-\beta)^n-28n^2\beta-20n^4\beta+\\ 15n^42^nBr\left(\frac{3n+1}{n}\right)^n(1-\beta)^n+38n^32^nBr\left(\frac{3n+1}{n}\right)^n(1-\beta)^n\\ +10n2^nBr\left(\frac{3n+1}{n}\right)^n(1-\beta)^n+32n^22^nBr\left(\frac{3n+1}{n}\right)^n(1-\beta)^n-\\ 2^nBr\beta\left(\frac{3n+1}{n}\right)^n(1-\beta)^n+56n^2+74n^3+31n^4+4n^4\beta^2\\ +8n^3\beta^2+4n^2\beta^2-4n\beta-44n^3\beta-4n^22^n\beta^3Br\left(\frac{3n+1}{n}\right)^n(1-\beta)^n\\ -56\beta Brn^22^n\left(\frac{3n+1}{n}\right)^n(1-\beta)^n+4\beta^2Brn2^n\left(\frac{3n+1}{n}\right)^n(1-\beta)^n-\\ 4n^4\beta^3Br2^n\left(\frac{3n+1}{n}\right)^n(1-\beta)^n-8n^3\beta^32^nBr\left(\frac{3n+1}{n}\right)^n(1-\beta)^n\\ +44\beta^2n^3Br2^n\left(\frac{3n+1}{n}\right)^n(1-\beta)^n-74\beta n^3Br2^n\left(\frac{3n+1}{n}\right)^n(1-\beta)^n\\ -31\beta n^4Br2^n\left(\frac{3n+1}{n}\right)^n(1-\beta)^n+20\beta^2n^4Br2^n\left(\frac{3n+1}{n}\right)^n(1-\beta)^n\end{array}} \tag{22}$$

For Newtonian fluids in the case of no-slip condition, Equation (22) reduces to $(768/(176+768Br))$, which is in agreement with the result given in literature [31]. Also, when $Br=0$, the common value $Nu=4.36$ is obtained.

In cooling process (negative values of the wall heat flux), there is a critical Brinkman number in which the Nusselt number tends to infinity:

$$Br_c=\frac{4n^2\beta^2-20n^2\beta-4n\beta+31n^2+12n+1}{\left(4n^2\beta^3-20n^2\beta^2+31n^2\beta-4n\beta^2+12n\beta-15n^2-8n+\beta-1\right)2^n\left(\frac{3n+1}{n}\right)^n(1-\beta)^n} \tag{23}$$

In general, entropy generation constitutes of two terms which are respectively due to thermal irreversibility and hydrodynamic irreversibility. Volumetric rate of entropy generation is [29]:

$$\begin{aligned}\dot{S}'''_{gen}&=\dot{S}'''_{HT}+\dot{S}'''_{FF}\\ &=\frac{k}{T^2}(\nabla T)^2+\frac{\tau_{rz}\left(-\frac{dV_z}{dr}\right)}{T}\\ &=\frac{k}{T^2}\left[\left(\frac{\partial T}{\partial z}\right)^2+\left(\frac{\partial T}{\partial r}\right)^2\right]+\frac{m}{T}\left(-\frac{dV_z}{dr}\right)^{n+1}\end{aligned} \tag{24}$$

If the following dimensionless entropy generation is as below:

$$N_s=\frac{\dot{S}'''_{gen}r_o^2}{k} \tag{25}$$

as well as Equations (2) and (18) are substituted into Equation (24), the dimensionless total entropy generation is obtained:

$$N_s=\frac{1}{\left(\theta+\frac{1}{\psi}\right)^2}\left[4\left(\frac{1+2^nBr(1-\beta)^{n+1}\left(\frac{3n+1}{n}\right)^n}{Pe}\right)^2+\left(\frac{\partial\theta}{\partial R}\right)^2\right] +\frac{Br\,2^{n-1}}{\left(\theta+\frac{1}{\psi}\right)}\left(-\frac{dV}{dR}\right)^{n+1} \tag{26}$$

where $\psi=q''D_h/(kT_w)$ is the dimensionless heat flux and $Pe=\rho c_p V_m D_h/k$ is the Peclet number. The dimensionless entropy generation due to conductive heat transfer is correspondingly expressed as:

$$N_{HT}=\frac{1}{\left(\theta+\frac{1}{\psi}\right)^2}\left[4\left(\frac{1+2^nBr(1-\beta)^{n+1}\left(\frac{3n+1}{n}\right)^n}{Pe}\right)^2+\left(\frac{\partial\theta}{\partial R}\right)^2\right] \tag{27}$$

Also, the dimensionless form of entropy generation contributed by fluid friction is written as:

$$N_{FF}=\frac{Br\,2^{n-1}}{(\theta+1/\psi)}\left(-\frac{dV}{dR}\right)^{n+1} \tag{28}$$

The average dimensionless entropy generation is defined as:

$$\bar{N}_s=\frac{1}{A_c}\int_{A_c}N_s\,dA_c=2\int_0^1 N_s\,R\,dR \tag{29}$$

3. RESULTS AND DISCUSSION

Effects of slip and viscous dissipation on heat transfer characteristics of fully-developed power-law fluid flows are studied in circular microchannels under an imposed constant wall heat flux. Figure 2a shows dimensionless

velocity profiles for $n = 0.5$ and different values of β. With increasing β, fluid velocity increases at the wall and decreases at the centerline; while, in contrast to no-slip condition, velocity gradient decreases at these regions. For large values of β, a plug-like velocity distribution is observed. Figure 2b represents dimensionless velocity distributions for $\beta = 0.3$ and various values of n. The core represents increased velocity with n, while its velocity gradient decreases. The velocity profile of pseudoplastic fluids become more uniform with n, while the opposite is true for dilatant fluids.

Figure 3 shows the Poiseuille number versus power-law index at different values of slip velocity. For a fixed slip velocity, with increase power-law index, Poiseuille number increases. Indeed, with increase power-law index, the value of velocity gradient at the wall decreases; but on the other hand, apparent viscosity of the fluid increases and since viscosity of the dilatant fluids are more than pseudo-plastic fluids, friction for dilatant fluids will be greater than pseudo-plastic fluids.

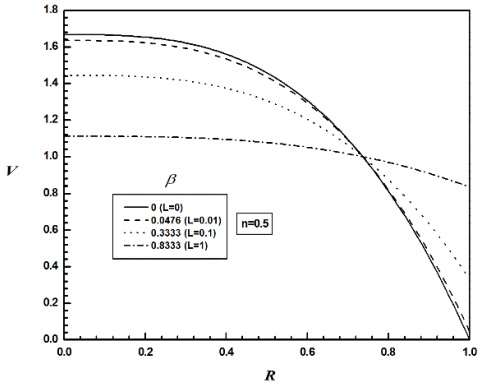

(a)

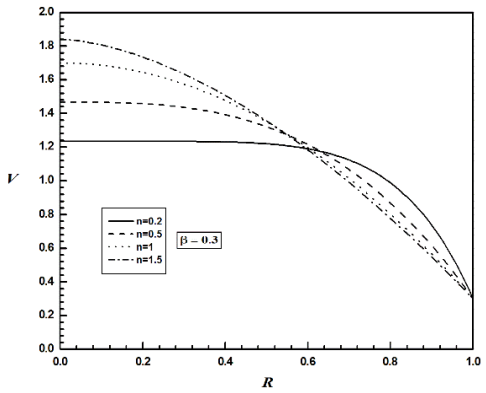

(b)

Figure 2. Dimensionless velocity profiles for various values of (a) β (b) n

In addition, with increasing slip velocity at the wall, Poiseuille number decreases because cohesion of the fluid in touch with the wall drastically reduces and so this process causes decreases of the friction between fluid and wall.

Figure 4 illustrates dimensionless temperature distributions for $n = 0.5$ and $n = 1.5$, and various values of β for two cases of the brinkman number (heating process). With increasing β, the dimensionless bulk fluid temperature increases. Since the surface velocity gradient and also viscous dissipation decrease; hence, a reduction in the temperature difference between the fluid and the wall is observed. With increasing Br, the temperature difference between the fluid and the surface is enhanced, due to viscous dissipation. It is clear that the overall behavior of dilatant fluids is similar to pseudoplastic fluids, but the former has much greater dimensionless temperatures.

In the absence of viscous dissipation (Figures 4a and 4c), the temperature field is more dominated by the advection mechanism. Moreover, viscous dissipation increases with increasing n; hence, for non-zero values of the Brinkman number (Figure 4d), the dimensionless temperature for dilatant fluids is higher than pseudoplastic fluids.

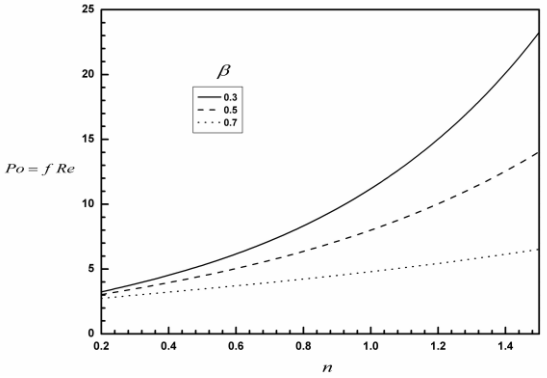

Figure 3. Poiseuille number versus power-law index

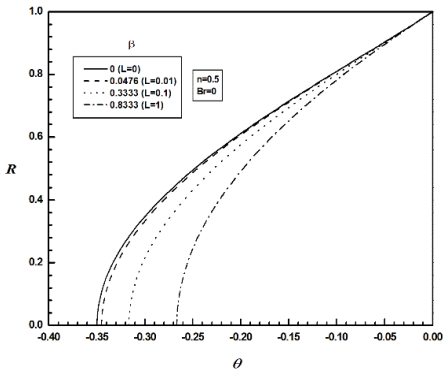

(a)

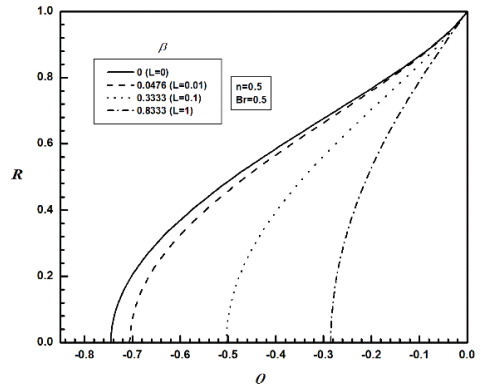

(b)

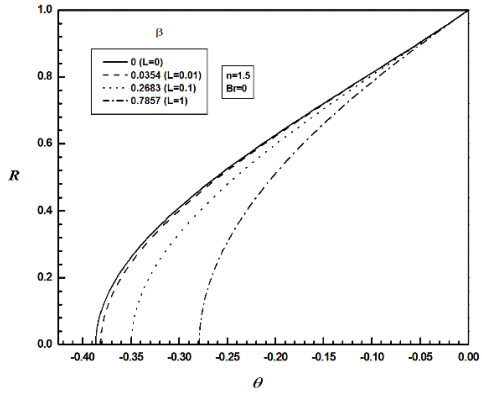

(c)

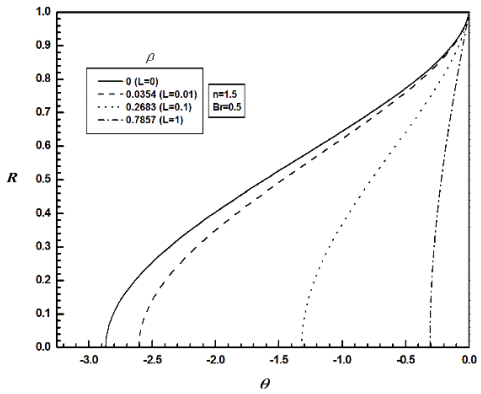

(d)

Figure 4. Dimensionless temperature profiles for various values of β ; (a),(b) pseudoplastics fluids and (c),(d) dilatant fluids

The temperature distributions of shear-thinning and shear-thickening fluids for various values of β are shown in Figures 5a and 5b for cooling process $(Br = -0.5)$. Negative dimensionless temperature always exist near the wall (the near-wall fluid temperature is higher than the surface temperature). For sufficiently large values of the slip coefficient, negative values of the dimensionless temperature are observed throughout the flow field; to be exact, there is a radial heat flux from the centerline towards the wall.

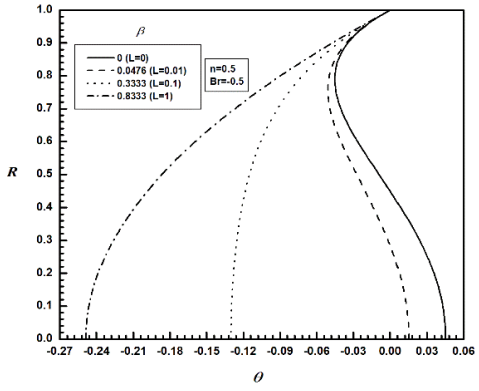

(a)

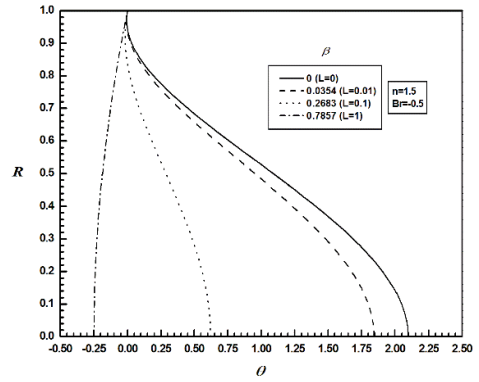

(b)

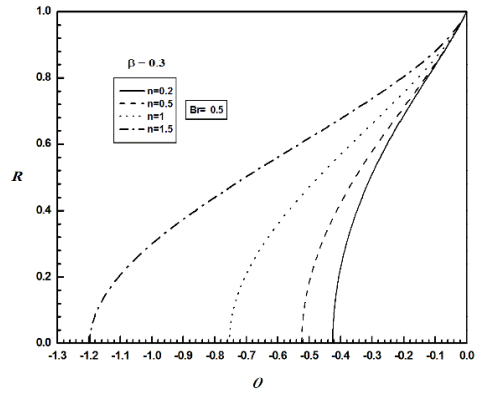

(c)

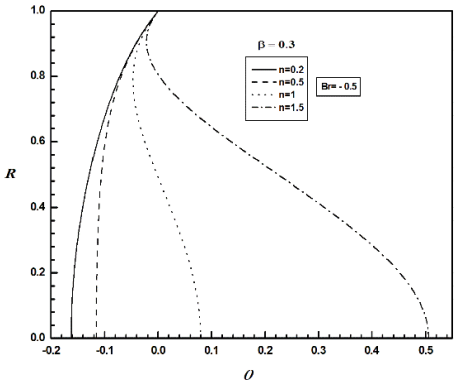

(d)

Figure 5. Dimensionless temperature profiles for various values of β and n for (a) pseudoplastics fluids, (b) dilatant fluids; (c) $Br = 0.5$, (d) $Br = -0.5$

In fact, with increasing slip coefficient, viscous dissipation decreases and critical Brinkman number increases; the dimensionless temperature will be negative.

As the slip coefficient reduces, positive values of the dimensionless temperature can be seen in the central portion of the channel (the core); i.e., the fluid temperature is smaller than the wall temperature. For heating process (Figure 5c), an increase in n leads to a decrease in the dimensionless bulk fluid temperature (larger dimensionless mean temperature with negative sign). This effect is especially significant for shear-thickening fluids. In cooling process (Figure 5d), for sufficiently high values of n, however, the fluid temperature (in the broad central area) is less than the wall temperature (positive values of the dimensionless temperature); because the advection mechanism dominates in this region and also for dilatant fluids the viscous dissipation effect at the wall is more than pseudoplastic fluids. Therefore, the wall temperature for dilatant fluids is higher than pseudoplastic fluids. Figures 6a and 6b show the Nusselt number as a function of the flow behavior index n, at various values of β for two different cases of the Brinkman number. The Nusselt number decreases with increasing n, because the smaller the value of n, the greater is the fluid velocity near the wall (see Figure 2b). However, if viscous dissipation is taken into account, this reduction is more tangible, so the Nusselt number is further reduced. In the case of $Br = 0$, for sufficiently large values of n, Nusselt number almost appreaches a constant value; because when there is no viscous dissipation, changes in the dimensionless temperature is not significant; so Nusselt number remains approximately constant. Nusselt number increases with β; this is due to the liquid slip in the wall-liquid interface which leads to higher velocity near the wall and hence to greater convection heat transfer. As can be seen in Figures 6c and 6d, Nusselt number is severely reduced (with negative sign) with increasing n and asymptotically converges to zero; because with increasing n, the bulk fluid temperature reduces.

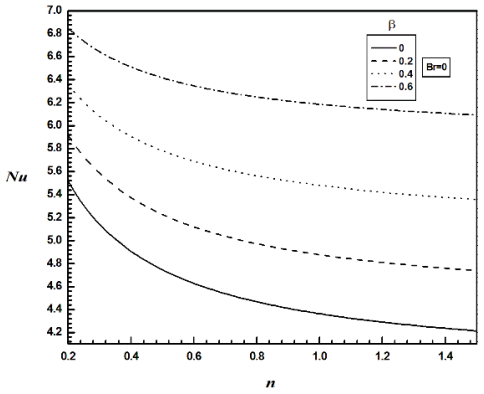

(a)

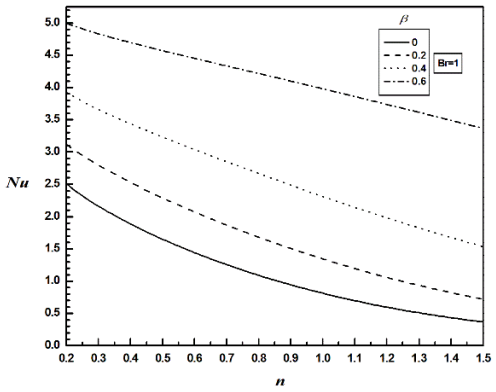

(b)

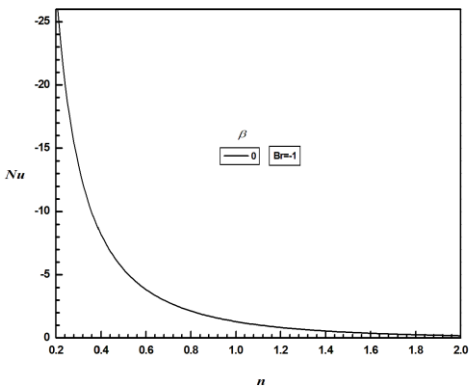

(c)

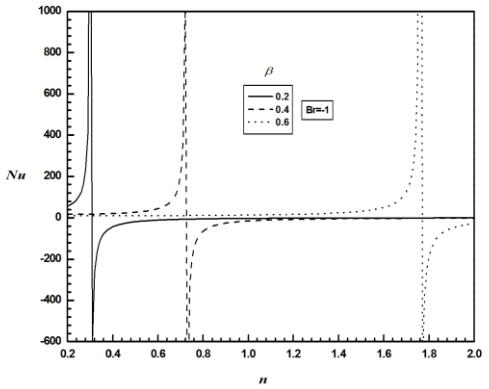

(d)

Figure 6. Nusselt number versus n and β; (a) Br=0; (b) Br=1; (c) n=0.5 ; (d) n=1.5

Some singularity points in Nusselt number are also observed in Figure 6d for each β; where, the mean fluid temperature reaches the wall temperature. For one particular value of the power law index in which $Br_c = -1$, a steep increase in Nusselt number is observed; the wall-fluid temperature difference decreases rapidly until it comes to a change of sign. Beyond the singular point, Nusselt number decreases rapidly.

Figure 7 shows that there are singular points in Nu for each β, in which, the bulk fluid temperature approaches the wall temperature $(Nu \to \infty)$.

It is noted that in higher values of β, the singularities occur at larger Br, because viscous dissipation at the wall and the fluid temperature decreases with β. Therefore, in higher values of Brinkman number, the bulk fluid temperature approaches to the wall temperature. These singular points, for instance, occur at $Br = -10.047$ ($\beta = 0.8333$) and $Br = -6.654$ ($\beta = 0.7857$) for $n = 0.5$ and $n = 1.5$, respectively. These singularities will be close to each other for smaller values of β. Nusselt number decreases for $-1 < Br < Br_c$; and a sharp decline is observed at the critical Brinkman number in which the temperature differences rapidly goes to zero until it comes to a change of sign. A rapid and gradual decline in the Nusselt number are observed, respectively, in the range of $Br_c < Br < 0$ and $0 < Br < 1$ (heating process). Related to Figure 8, an increase in β results in a reduction of the surface velocity gradient and also a reduction in the rate of thermal irreversibility for both shear-thinning and shear-thickening fluids.

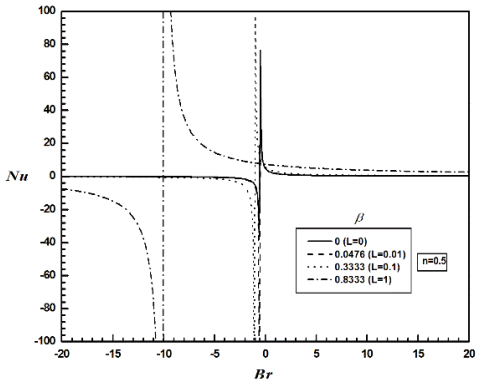

(a)

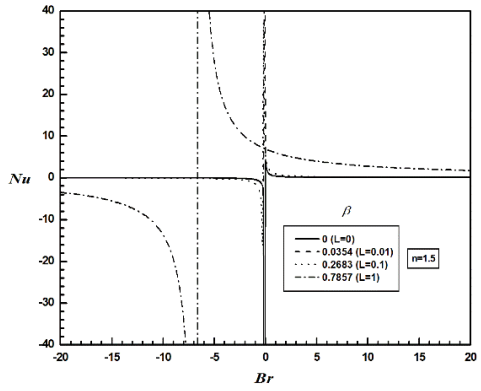

(b)

Figure 7. Nusselt number versus Br for different values of β ; (a) n=0.5, (b) n=1.5

Actually entropy generation due to heat transfer depends on both axial and radial diffusion. However, it is much more affected by radial diffusion.

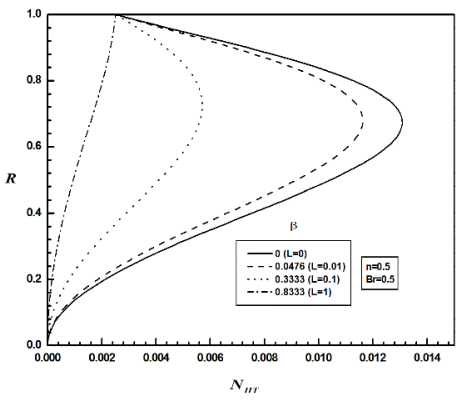

(a)

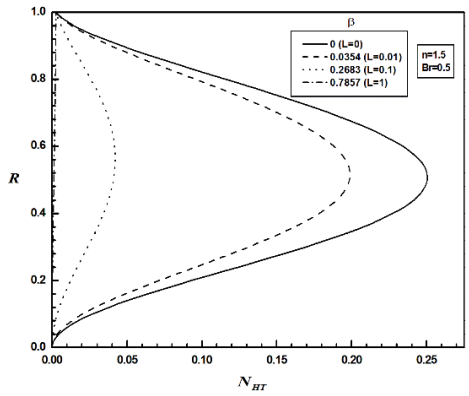

(b)

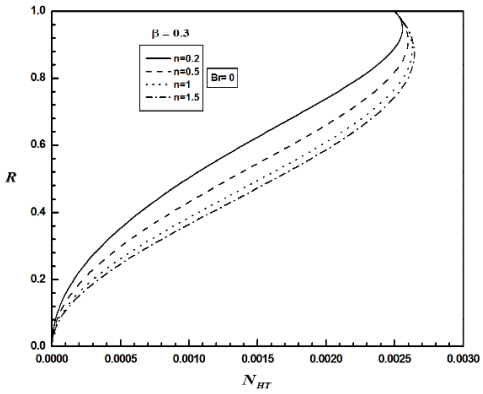

(c)

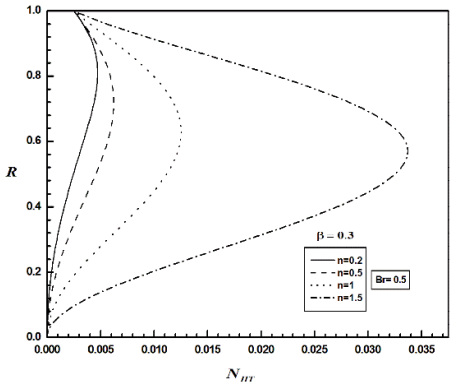

(d)

Figure 8. Dimensionless entropy generation from heat transfer for various values of β and n; (a) n=0.5, (b) n=1.5; (c) Br=0, (d) Br=0.5

An increase in the flow behavior index (also Brinkman number) leads to enhance the dimensionless radial temperature gradient and also the dimensionless entropy generation due to heat transfer.

In Figure 9, with increasing β, the dimensionless entropy generation due to fluid friction is reduced; because with increase of β, the velocity gradient at the wall and therefore the viscous dissipation are decreased for both dilatant and pseudoplastic fluids.

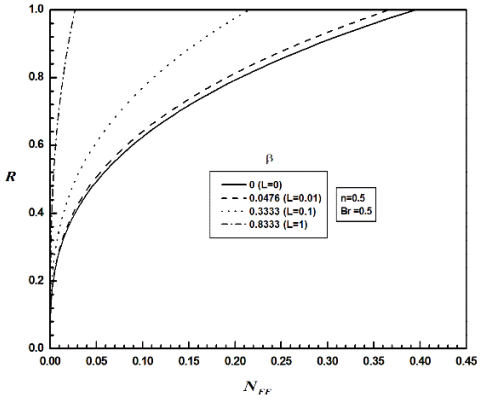

(a)

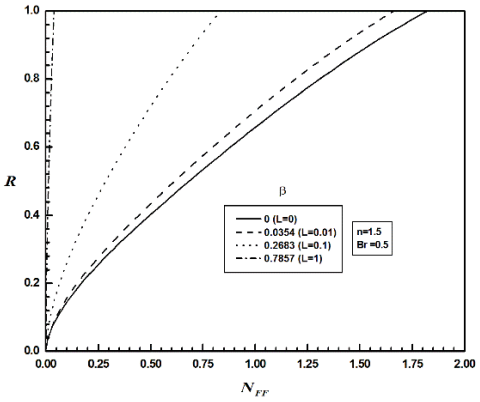

(b)

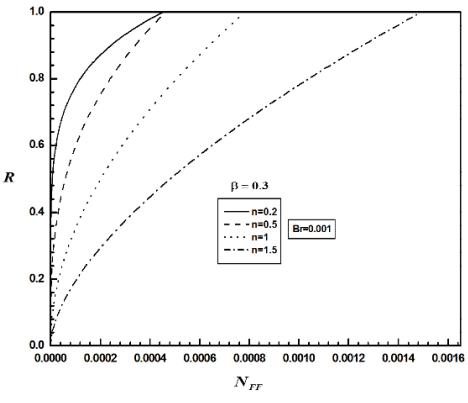

(c)

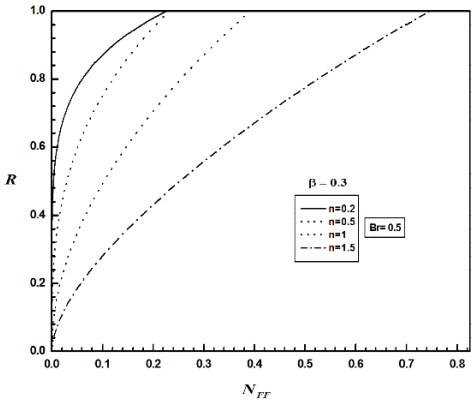

(d)

Figure 9. Dimensionless entropy generation from fluid friction for various values of β and n; (a) n=0.5, (b) n=1.5; (c) Br=0, (d) Br=0.5

The maximum value of N_{FF} occurs at the wall (because of maximum velocity gradient) and is zero at the centerline.

Also, higher values of Br (for constant n) result in higher values of N_{FF}, since viscous dissipation at the wall increases with Br.

4. CONCLUDING REMARKS

According to this analytic study, Brinkman number, slip coefficient and flow behavior index mainly affect the flow field. The conclusions are:

i. The wall velocity gradient decreases with increasing the slip coefficient, resulting in smaller values of viscous heating.

ii. Pseudoplastics exhibit lower velocities than dilatants near the centerline (the opposite behavior is observed near the wall). A plug-like velocity distribution may be attained for sufficiently small values of the flow behavior index (at a fixed mass flow rate).

iii. Poiseuille number decreases when slip velocity increases at the wall which is due to the reduction of friction between fluid and wall of the microchannel. Also, Poiseuille number for dilatant fluids is more than pseudoplastic (because of the higher apparanrt viscosity of dilatant fluids).

iv. In heating mode, the fluid-wall temperature difference decreases with the slip coefficient (for a fixed n); similar behavior may not be observed in cooling.

v. Effect of increasing the flow behavior index is to broaden temperature profiles for both surface heating and cooling, resulting in enlarging the temperature difference between the fluid and the wall.

vi. In cooling mode, the bulk fluid temperature may be greater or smaller than the wall temperature depending on the value of the flow behavior index as well as the slip coefficient. For sufficiently large values of the slip coefficient or sufficiently small values of the flow behavior index, the bulk fluid temperature is greater than the wall temperature.

vii. The higher value of the Brinkman number, the lesser will be the conduction of heat produced by viscous dissipation and hence larger the temperature rise.

viii. The fully-developed Nusselt number increases with the slip coefficient (and decreases with the flow behavior index and the Brinkman number) in heating mode.

ix. Variations of Nu with Br as well as n exhibit singularities which occur in the cooling range; in these singular points, the Nusselt number tends to infinity. The critical Brinkman number associated with this particular situation depends on the flow behavior index and the slip coefficient.

x. When viscous dissipation is negligible, for sufficiently large values of the power-law index, the Nusselt number remains almost unchanged with the flow behavior index.

xi. The critical Brinkman number decreases with increasing power-law index, while it increases with the slip coefficient.

xii. Entropy generation is enhanced by decreasing the slip coefficient or increasing the power-law index. Dilatants are more irreversibility than pseudoplastics.

xiii. Total entropy generation increases with increasing both power-law index and Brinkman number, whereas decreases with the existence of slip condition.

xiv. For shear-thickening fluids, the rate of entropy generation from fluid friction is more than that of entropy generation from heat transfer; while the reverse is true for shear-thinning fluids.

4. REFERENCES

1. Byun, D., Kim, J., Ko, H.S. and Park, H.C., "Direct measurement of slip flows in superhydrophobic microchannels with transverse grooves", ***Physics of Fluids***, Vol. 20, No. 11, (2008), 113601.

2. Tretheway, D.C. and Meinhart, C.D., "A generating mechanism for apparent fluid slip in hydrophobic microchannels", ***Physics of Fluids***, Vol. 16, No. 5, (2004), 1509-1515.

3. Chun, M.-S. and Lee, S., "Flow imaging of dilute colloidal suspension in pdms-based microfluidic chip using fluorescence microscopy", ***Colloids and Surfaces A: Physicochemical and Engineering Aspects***, Vol. 267, No. 1, (2005), 86-94.
4. Sparrow, E. and Haji-Sheikh, A., "Velocity profile and other local quantities in free-molecule tube flow", ***The Physics of Fluids***, Vol. 7, No. 8, (1964), 1256-1261.
5. Roy, P., Anand, N. and Banerjee, D., "Liquid slip and heat transfer in rotating rectangular microchannels", ***International Journal of Heat and Mass Transfer***, Vol. 62, (2013), 184-199.
6. Wu, Y., Cai, M., Li, Z., Song, X., Wang, H., Pei, X. and Zhou, F., "Slip flow of diverse liquids on robust superomniphobic surfaces", ***Journal of Colloid and Interface Science***, Vol. 414, (2014), 9-13.
7. Afonso, A., Alves, M. and Pinho, F., "Analytical solution of mixed electro-osmotic/pressure driven flows of viscoelastic fluids in microchannels", ***Journal of Non-Newtonian Fluid Mechanics***, Vol. 159, No. 1, (2009), 50-63.
8. Ashorynejad, H., Javaherdeh, K., Sheikholeslami, M. and Ganji, D., "Investigation of the heat transfer of a non-newtonian fluid flow in an axisymmetric channel with porous wall using parameterized perturbation method (PPM)", ***Journal of the Franklin Institute***, Vol. 351, No. 2, (2014), 701-712.
9. Ng, C.-O. and Qi, C., "Electroosmotic flow of a power-law fluid in a non-uniform microchannel", ***Journal of Non-Newtonian Fluid Mechanics***, Vol. 208, No., (2014), 118-125.
10. Bharti, R.P., Harvie, D.J. and Davidson, M.R., "Electroviscous effects in steady fully developed flow of a power-law liquid through a cylindrical microchannel", ***International Journal of Heat and Fluid Flow***, Vol. 30, No. 4, (2009), 804-811.
11. Dehkordi, A.M. and Mohammadi, A.A., "Transient forced convection with viscous dissipation to power-law fluids in thermal entrance region of circular ducts with constant wall heat flux", ***Energy Conversion and Management***, Vol. 50, No. 4, (2009), 1062-1068.
12. Barkhordari, M. and Etemad, S.G., "Numerical study of slip flow heat transfer of non-newtonian fluids in circular microchannels", ***International Journal of Heat and Fluid Flow***, Vol. 28, No. 5, (2007), 1027-1033.
13. Tyagi, V., "Laminar forced convection of a dissipative fluid in a channel", ***ASME J. Heat Transfer***, Vol. 88, No. 2, (1966), 161-167.
14. Rao, I. and Rajagopal, K., "The effect of the slip boundary condition on the flow of fluids in a channel", ***Acta Mechanica***, Vol. 135, No. 3, (1999), 113-126.
15. Aydin, O., "Effects of viscous dissipation on the heat transfer in forced pipe flow. Part 1: Both hydrodynamically and thermally fully developed flow", ***Energy Conversion and Management***, Vol. 46, No. 5, (2005), 757-769.
16. Tso, C., Sheela-Francisca, J. and Hung, Y.-M., "Viscous dissipation effects of power-law fluid flow within parallel plates with constant heat fluxes", ***Journal of Non-Newtonian Fluid Mechanics***, Vol. 165, No. 11, (2010), 625-630.
17. Lawal, A. and Mujumdar, A., "The effects of viscous dissipation on heat transfer to power law fluids in arbitrary cross-sectional ducts", ***Warme-und Stoffübertragung***, Vol. 27, No. 7, (1992), 437-446.
18. Hung, Y.M., "Analytical study on forced convection of nanofluids with viscous dissipation in microchannels", ***Heat Transfer Engineering***, Vol. 31, No. 14, (2010), 1184-1192.
19. Hung, Y.-M., "A comparative study of viscous dissipation effect on entropy generation in single-phase liquid flow in microchannels", ***International Journal of Thermal Sciences***, Vol. 48, No. 5, (2009), 1026-1035.
20. Chen, G. and Tso, C., "Effects of viscous dissipation on forced convective heat transfer in a channel embedded in a power-law fluid saturated porous medium", ***International Communications in Heat and Mass Transfer***, Vol. 38, No. 1, (2011), 57-62.
21. Moghadam, A.J., "Thermal characteristics of time-periodic electroosmotic flow in a circular microchannel", ***Heat and Mass Transfer***, Vol. 51, No. 10, (2015), 1461-1473.
22. Moghadam, A.J., "Exact solution of electroviscous flow and heat transfer in a semi-annular microcapillary", ***Journal of Heat Transfer***, Vol. 138, No. 1, (2016), 011702.
23. Moghadam, A.J., "Electrokinetic-driven flow and heat transfer of a non-newtonian fluid in a circular microchannel", ***Journal of Heat Transfer***, Vol. 135, No. 2, (2013), 021705.
24. Mohammadi, M.-R. and Moghadam, A.J., "Heat transfer and entropy generation analysis of bingham plastic fluids in circular microchannels", ***Journal of Thermal Science and Engineering Applications***, Vol. 7, No. 4, (2015), 041019.
25. Sarabandi, A.-H. and Moghadam, A.J., "Thermal analysis of power-law fluid flow in a circular microchannel", ***Journal of Heat Transfer***, Vol. 139, No. 3, (2017), 032401.
26. Larrodé, F.E., Housiadas, C. and Drossinos, Y., "Slip-flow heat transfer in circular tubes", ***International Journal of Heat and Mass Transfer***, Vol. 43, No. 15, (2000), 2669-2680.
27. Moghadam, A.J. and Akbarzadeh, P., "Time-periodic electroosmotic flow of non-newtonian fluids in microchannels", ***International Journal of Engineering-Transactions B: Applications***, Vol. 29, No. 5, (2016), 706-712.
28. Moghadam, A.J., "Two-fluid electrokinetic flow in a circular microchannel (research note)", ***International Journal of Engineering-Transactions A: Basics***, Vol. 29, No. 10, (2016), 1469-1474.
29. Bejan, A., "Entropy generation through heat and fluid flow, Wiley, (1982).
30. Bejan, A., "A study of entropy generation in fundamental convective heat transfer", ***Journal of Heat Transfer***, Vol. 101, No. 4, (1979), 718-725.
31. Bejan, A., "Entropy generation minimization: The new thermodynamics of finite-size devices and finite-time processes", ***Journal of Applied Physics***, Vol. 79, No. 3, (1996), 1191-1218.
32. Mah, W.H., Hung, Y.M. and Guo, N., "Entropy generation of viscous dissipative nanofluid flow in microchannels", ***International Journal of Heat and Mass Transfer***, Vol. 55, No. 15, (2012), 4169-4182.
33. Tan, L. and Chen, G., "Analysis of entropy generation for a power-law fluid in microchannels", ***ASME Paper No. MNHMT2013-22159***, (2013).
34. Hung, Y.-M., "Viscous dissipation effect on entropy generation for non-newtonian fluids in microchannels", ***International Communications in Heat and Mass Transfer***, Vol. 35, No. 9, (2008), 1125-1129.
35. Mahmud, S. and Fraser, R.A., "Second law analysis of forced convection in a circular duct for non-newtonian fluids", ***Energy***, Vol. 31, No. 12, (2006), 2226-2244.
36. Mahmud, S. and Fraser, R.A., "Inherent irreversibility of channel and pipe flows for non-newtonian fluids", ***International Communications in Heat and Mass Transfer***, Vol. 29, No. 5, (2002), 577-587.
37. Mahmud, S. and Fraser, R.A., "The second law analysis in fundamental convective heat transfer problems", ***International Journal of Thermal Sciences***, Vol. 42, No. 2, (2003), 177-186.
38. Escandón, J., Bautista, O. and Méndez, F., "Entropy generation in purely electroosmotic flows of non-newtonian fluids in a microchannel", ***Energy***, Vol. 55, (2013), 486-496.

39. Bird, R.B., Stewart, W.E. and Lightfoot, E.N., "Transport phenomena, John Wiley & Sons, (2007).
40. Chhabra, R.P. and Richardson, J.F., "Non-newtonian flow and applied rheology: Engineering applications, Butterworth-Heinemann, (2011).
41. Ferrás, L.L., Nóbrega, J.M. and Pinho, F.T., "Analytical solutions for channel flows of phan-thien–tanner and giesekus fluids under slip", ***Journal of Non-Newtonian Fluid Mechanics***, Vol. 171, (2012), 97-105.
42. Pereira, G., "Effect of variable slip boundary conditions on flows of pressure driven non-newtonian fluids", ***Journal of Non-Newtonian Fluid Mechanics***, Vol. 157, No. 3, (2009), 197-206.
43. Tan, D. and Liu, Y., "Combined effects of streaming potential and wall slip on flow and heat transfer in microchannels", ***International Communications in Heat and Mass Transfer***, Vol. 53, (2014), 39-42.

Slip Velocity in Flow and Heat Transfer of Non-newtonian Fluids in Microchannels

A. H. Sarabandi, A. Jabari Moghadam

Mechanical Engineering Department, Shahrood University of Technolgy, Shahrud, Iran

P A P E R I N F O

Paper history:
Received 22 December 2016
Received in revised form 02 March 2017
Accepted 21 April 2017

Keywords:
Heat Transfer
Non-Newtonian Fluids
Slip
Brinkman Number
Analytic Solution
Entropy Generation
Nusselt Number

چکیده

جریان آرام توسعه یافته حالت پایدار سیالات غیرنیوتنی مدل پاورلا در میکروکانال گرد با شرط سرعت لغزشی و در وضعیت شار ثابت دیوار بررسی می‌شود. اثر لغزش و نیز پارامترهای کلیدی هیدرودینامیکی و گرمایی بر روی انتقال گرما و تولید انتروپی مطالعه می‌گردد. از نتایج چنین برمی‌آید که افزایش عدد برینکمن و شاخص رفتاری جریان، هردو به افزایش تولید انتروپی و کاهش عدد ناسلت منجر می‌شوند. در فرآیند گرمایش، اختلاف دمای بین سیال و دیوار، با افزایش ضریب لغزش کاهش می‌یابد؛ روند مشابهی ممکن است برای فرآیند سرمایش مشاهده گردد، که به محدوده ضریب لغزش و نیز عدد برینکمن بستگی دارد. افزایش ضریب لغزش، هم به افزایش عدد ناسلت و هم عدد بیژن منجر می‌گردد، درحالی‌که موجب کاهش تولید انتروپی می‌شود. به ازای مقدار بخصوصی از ضریب لغزش، با افزایش عدد برینکمن و یا شاخص رفتاری جریان، عدد ناسلت به مقدار خاصی میل می‌کند. افزایش شاخص رفتاری جریان یا کاهش ضریب لغزش، سبب زیادشدن میانگین تولید انتروپی می‌شود.

***doi**: 10.5829/ije.2017.30.07a.15*